New short-range biopyribole polysomes from the Lepontine Alps, Switzerland

Bernard H. Grobéty*

Institut für Mineralogie und Petrographie, Eidgenössische Technische Hochschule,
8092 Zurich, Switzerland

Abstract

Retrograde hydration of anthophyllite found in ultramafic lenses of the Lepontine Alps, southern Switzerland, resulted in the formation of talc and additional ordered and disordered biopyribole polysomes. Among the ordered sequences, 13 new short-range biopyribole polysomes were discovered using high-resolution transmission electron microscopy (HRTEM). The most significant new polysomes are ordered sequences of quadruple-, triple-, and double-chains: (42), (432), (4323), and the first pyribole polysome with a composition between pyroxene and amphibole, (2111). Up to 40 unfaulted repetitions of these sequences are present in several grains. More complex polysomes like (423232) occur as intermediate steps in the formation of shorter polysomes, e.g., the polysome (332). The polysome (42) is the first short-range polysome, for which each step of the formation mechanism is documented. The precursors are disordered sequences countering quadruple- and double-chains, which are formed through coherent zipper transformations from anthophyllite. The disordered sequences are subsequently transformed to the ordered polysome (42). The multiple-step reaction path strongly suggests that energy minimization is partly responsible for the appearance of some of the short-range polysomes.

The major element chemistry of the short-range polysomes, determined by analytical electron microscopy (AEM), is identical to that of the macroscopically occurring biopyriboles, excluding, therefore, a stabilization of the short-range polysomes by additional elements.

The ordering of (010) stacking faults in enstatite connecting partial dislocations, each with a $\frac{1}{4}[100] \pm \frac{1}{3}[001]$ displacement component, led to the formation of the (2111) polysome. Along the fault plane, pairs of pyroxene I beams are juxtaposed and transform subsequently to amphibole chains. The composition of the (2111) polysome is colinear with the coexisting enstatite and anthophyllite.

Introduction

High concentrations of planar defects are characteristic of asbestiform amphiboles. Transmission electron microscopy (TEM) studies of these faults show that they contain chains that are more than two SiO_4 tetrahedra wide (Chisholm 1973; Buseck and Iijima 1974; Hutchison et al. 1975). Polysomatism, a concept from modular crystallography, considerably simplifies the description of chain silicates and emphasizes their structural relationship (Thompson 1978, 1981; for a review, see Veblen 1991). The amphibole structure can be represented as an assembly of pyroxene-like (P) and mica-like (M) slabs (= modules) cut along (010) planes and stacked together along their common b axis in a PM sequence (see Fig. 3, Thompson 1978). A triple-chain structure is composed of one P module alternating with two M modules. All intermediate structures, characterized by different mod-

ule ratios and stacking arrangements, form a polysomatic series defined by the end-members pyroxene and mica. Thompson named this polysomatic mineral group biopyriboles, a revival of a collective field term for micas (biotite), pyroxenes, and amphiboles introduced by Johannsen (1911). The first synthetic ordered wide-chain structure, a phase containing only triple-chains, was synthesized hydrothermally by Drits et al. (1974). The first nonclassical natural biopyriboles, jimthompsonite (Jt) and chesterite (Che), were discovered in a talc quarry near Chester, Vermont (Veblen and Burnham 1978a, 1978b). Jimthompsonite is a triple-chain silicate, similar to the structure synthesized by Drits et al. (1974). Chesterite is the first mixed-chain biopyribole, with alternating double- and triple-chains along its b axis. Veblen and Burnham (1978a) interpreted these new minerals as intermediate phases in the retrograde alteration of anthophyllite (Ath) to talc (Tlc). Along with the macroscopically occurring jimthompsonite and chesterite, the ultramafic samples contained partly reacted anthophyllite with disordered wide-chain polysomes. Among the disordered

* Present address: Geologi Institut, C.F. Møllersallé 120, DK-8000, Århus C, Denmark.

regions, small areas with ordered complex superstructures, called short-range polysomes, were found (Veblen and Buseck 1979). Probability calculations showed that a formation of these short-range polysomes through a random process is very unlikely. The propagation of wide-chains around screw dislocations in anthophyllite was proposed as a possible formation mechanism of ordered sequences (Veblen and Buseck 1979), although such dislocations were not observed.

Natural wide-chain pyriboles do not occur only in amphibolite facies, metasomatic altered ultramafic rocks. Wide-chain Ca-bearing pyriboles were found in low-temperature hydrothermal veins (Yau et al. 1986) and in the alteration halo of a skarn ore deposit (Akai 1980). Wide-chain material formed as a low-temperature weathering product of enstatite (Eggleton and Boland 1982). Wide chains are characteristic of all asbestiform amphiboles (Veblen 1980; Cressey et al. 1982; Dorling and Zussman 1987; Ahn and Buseck 1991) and for hydrothermally synthesized amphiboles (Maresch and Czank 1988; Ahn et al. 1991). Recently Droop (1994) described the prograde development of jimthompsonite, clinojimthompsonite, chesterite, and clinochesterite in Lewisian ultramafic rocks.

Retrograde alteration of pyroxenes in different geological environments may also produce disordered intergrown polysomes (Veblen and Buseck 1981; Nakajima and Ribbe 1980, 1981). However, no ordered polysomes containing pyroxene chains have been found thus far in nature.

To date, no attempt has been made to determine experimentally the thermodynamic characteristics of these new biopyribole polysomes. Their stability was investigated using energy minimization techniques (Abbott and Burnham 1991) and an axial-next-nearest-neighbor-Ising (ANNNI) model (Price and Yeomans 1986). The results of these investigations suggest that jimthompsonite is the phase most likely to have a stability field.

In this paper, transmission electron microscopy (TEM) observations of new short-range polysomes from the Lepontine Alps, Switzerland, are presented. Several possible formation mechanisms for short-range polysomes are discussed.

GEOLOGICAL SETTING AND SAMPLE DESCRIPTION

Ultramafic lenses, ranging from several tens to some hundreds of meters in thickness, are common in the pre-Mesozoic basement of the Lepontine Alps, Ticino, Switzerland. The studied samples were collected from a lens in Val Cramosina (Mg29a, Mg collection, V. Trommsdorff, ETH Zurich), and from a small ultramafic body near Alpe Bena in the upper Valle Maggia (BL8, Stoll 1990), both situated in the northern part of the Lepontine. Plagioclase, two-mica gneisses, and Mesozoic carbonate rocks surround the lenses at both localities. Both were metamorphosed to amphibolite grade during the Alpine orogeny, which led to the formation of kyanite, staurolite, and garnet in the Paleozoic basement rocks (Köppel et al. 1980).

The paragenesis anthophyllite (Ath) + talc (Tlc) + magnesite (Mgs) ± enstatite (En) ± forsterite (Fo) is a common assemblage in the ultramafic bodies of the Central Alps. The genetic relationship between enstatite and anthophyllite in these rocks is disputed. The assemblage En + Tlc is present in the core, whereas Ath + Tlc are present in the outer parts of the Lepontine. Trommsdorff (1983) interpreted this distribution as a prograde replacement of Ath by En + Tlc because of an increase in temperature toward the center of the Lepontine. The latter interpretation is possible only with a negative P-T slope for the reaction Ath → En + Tlc, which is inconsistent with most experimental data (Berman et al. 1986). Berman et al. (1986) explained the formation of En + Tlc as a result of a pressure increase, possibly related to the Eo-Alpine subduction of Penninic oceanic crust. Anthophyllite formed later as a retrograde product from enstatite during the uplift of the Lepontine (Pfeifer 1978). In the rocks of the central part of the Lepontine En + Tlc survived the decompression because of the higher Mg content of the rocks. Evans and Trommsdorff (1974) showed that the location of the fluid-absent reaction En + Tlc → Ath in P-T space is very sensitive to variations of X_{Mg} in the rock. A slight increase in X_{Mg} of the participating phases shifts the equilibrium to lower pressures and higher temperatures and therefore extends the stability field for En + Tlc. TEM observations presented below support the retrograde sequence En + Tlc → Ath and decompression as the formation mechanism of anthophyllite.

The anthophyllite crystals have fibrous habit and coexist with flaky talc. Anthophyllite is replaced by very fine-grained secondary talc along grain boundaries and cleavage planes. Occasionally anthophyllite is also overgrown by magnesite. No optically visible enstatite was found, although this mineral is present in other lenses located near Val Cramosina (Val d'Efra, Cima di Gagnone; Evans and Trommsdorff 1974). Additionally, the sample from Val Cramosina contains olivine, the only macroscopic relict of the primary peridotitic assemblage. Late, cross-cutting antigorite veinlets replace both olivine and anthophyllite. The anthophyllite crystals are strongly striated in all three samples. The striations parallel to (010) are typical for anthophyllite containing intergrowths of wide-chain pyriboles (Veblen and Burnham 1978a). A previous HRTEM investigation of anthophyllite from the nearby Val d'Agro confirmed the presence of chain-width faults (Nissen et al. 1980).

Estimates of temperatures and pressures for the main Alpine metamorphism determined in the surrounding gneisses (Frey 1974; Frey et al. 1980; Klaper 1982) are approximately 600 ± 50 °C and 4–6 kbar. Temperature estimates for the formation of the wide-chain biopyriboles, using the method of Schumacher and Czank (1987) based on Mg-Fe partitioning between different polysomes, give 500–600 °C. The formation of the wide-chain pyriboles occurred, therefore, during the retrograde stage

TABLE 1. New polysomes found at Alpe Bena and Val Cramosina

Sequence	Obs. repeats	Prob.*	Stoichiometry	Repeat length (nm)	Max. Symm.**	Occurrence
2233	6	5.41×10^{-6}	M_3P_2	4.5	$P2_1/a$	Alpe Bena
$(2)^6(3)^6$	7	2.25×10^{-21}	M_3P_2	13.5	Pa	Alpe Bena
24	40	3.67×10^{-23}	M_2P	2.7	$P2_1ma$	Val Cramosina
234	49	3.45×10^{-67}	M_2P	4.05	Pa	Val Cramosina
2343	6	2.15×10^{-8}	M_2P	5.4	$P2_1ma$	Val Cramosina
233	11	3.33×10^{-8}	M_5P_3	3.6	$P2_1ma$	Val Cramosina
423232	26	2.04×10^{-64}	M_5P_3	7.2	$P2_1ma$	Val Cramosina
423322	3	7.21×10^{-5}	M_5P_3	7.2	Pa	Val Cramosina
43221222	3	1.38×10^{-6}	M_5P_3	7.2	Pa	Val Cramosina
$324(2)^3324(2)^5$	3	4.6×10^{-9}	$M_{10}P_7$	15.3	Pa	Val Cramosina
$424233(2)^3324(2)^{15}$	3	3.29×10^{-16}	$M_{41}P_{32}$	32.8		Alpe Bena
$32324233(2)^6(32)^3(2)^{12}$	3	1.70×10^{-17}	$M_{41}P_{32}$	32.8		Alpe Bena
21	4	5.01×10^{-2}	MP_2	1.35	$A2_1ma$	Val Cramosina
2111	46	1.62×10^{-43}	MP_4	2.25	$A2_1ma$	Val Cramosina
322212	5	1.93×10^{-8}	MP	5.4	Pa	Val Cramosina

* Probability for the formation of a polysome through a random process (Veblen and Buseck 1979); for explanation see text.
** Symmetry assuming orthopyroxene stacking $(++--)$ (Thompson 1981).

of the main Alpine metamorphism, and it was not the result of subsequent low-temperature alteration.

EXPERIMENTAL METHODS AND BIOPYRIBOLE TERMINOLOGY

Ion-thinned basal (001) sections of anthophyllite were studied using high-resolution transmission electron microscopy (HRTEM). The carbon-coated discs were mounted on a double-tilt stage and examined in a JEOL 200CX and a Philips 420ST microscope operated at 200 and 120 keV, respectively. Analytical electron microscopy (AEM) was performed on the latter instrument as described by Livi and Veblen (1987). Primary magnifications varied between 200 000x and 450 000x. Images were recorded near Scherzer defocus values. Image interpretation follows that of Veblen and Buseck (1979).

The compositions of the biopyriboles were analyzed in polished thin sections with a CAMECA SX 50 electron microprobe using an acceleration voltage of 15 keV and a beam current of 20 nA. The standards were natural

oxides and silicates. The data were corrected for absorption effects with a PAP-enhanced ZAF method provided by CAMECA (Pouchon and Pichoir 1984).

The terminology used in the present paper follows that given by Veblen and Buseck (1980). The polysomatic description of chain silicates is based on two modules represented by (010) slabs of the pyroxene-like and the mica-like structures (P and M modules; Thompson 1978). Individual chains contain a variable number of M modules bounded by one-half P module on each side (e.g., amphibole = ... ½ P M ½ P ½ P M ½ P ... = ... MPMP ...). The width of an individual chain is given by its total number of modules, which is equal to the number of SiO_4 subchains of that chain (width of a pyroxene chain = 1; width of an amphibole chain = 2, etc.).

Veblen and Buseck (1980) used the term zippers for wide chains within a matrix of amphibole. Zippers, in classical crystallographic terms, are Wadsley defects. In this paper, sequences containing several wide chains within an anthophyllite matrix will also be called zippers. Wide chains are usually very extended in the a and c directions and, therefore, can be represented as two-dimensional slabs.

A sequence of chains is called ordered when the observable repetitions of the basic unit fulfill the statistical criterion given by Veblen and Buseck (1979):

$$p = \frac{n_1!n_2!n_3! \ldots}{n_1! + n_2! + n_3! \ldots}$$

where n_i = number of chains with width i in the repeating unit.

Sequences are considered to be nonrandom for values of $p < 0.001$. Ordered short-range polysomes are designated by the chain sequence of their basic repeating unit placed in parentheses [e.g., jimthompsonite, a triple-chain silicate, is given as (3), chesterite is (32)]. An individual chain or a chain group that occurs several consecutive times within a repeating unit may be represented by indicating the number of repetitions as a superscript [e.g.,
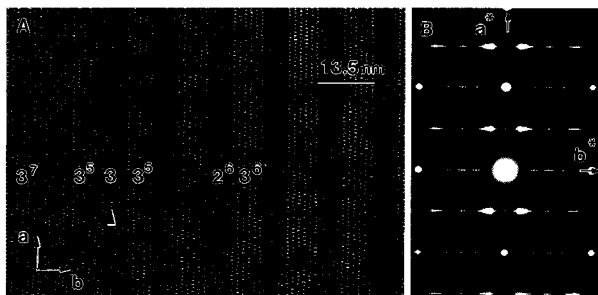

FIGURE 1. (A) The [001] high-resolution electron transmission microscopy (HRTEM) image and (B) selected-area electron diffraction (SAED) pattern of the (2^63^6) polysome. The numbers of individual chains in some lamellae are indicated. Chain-width faults, such as the isolated triple-chain slab in a double-chain lamella (arrow), are discussed in the text. All subsequent HRTEM images have the same crystallographic orientation as indicated in Figure 2A, unless otherwise indicated.
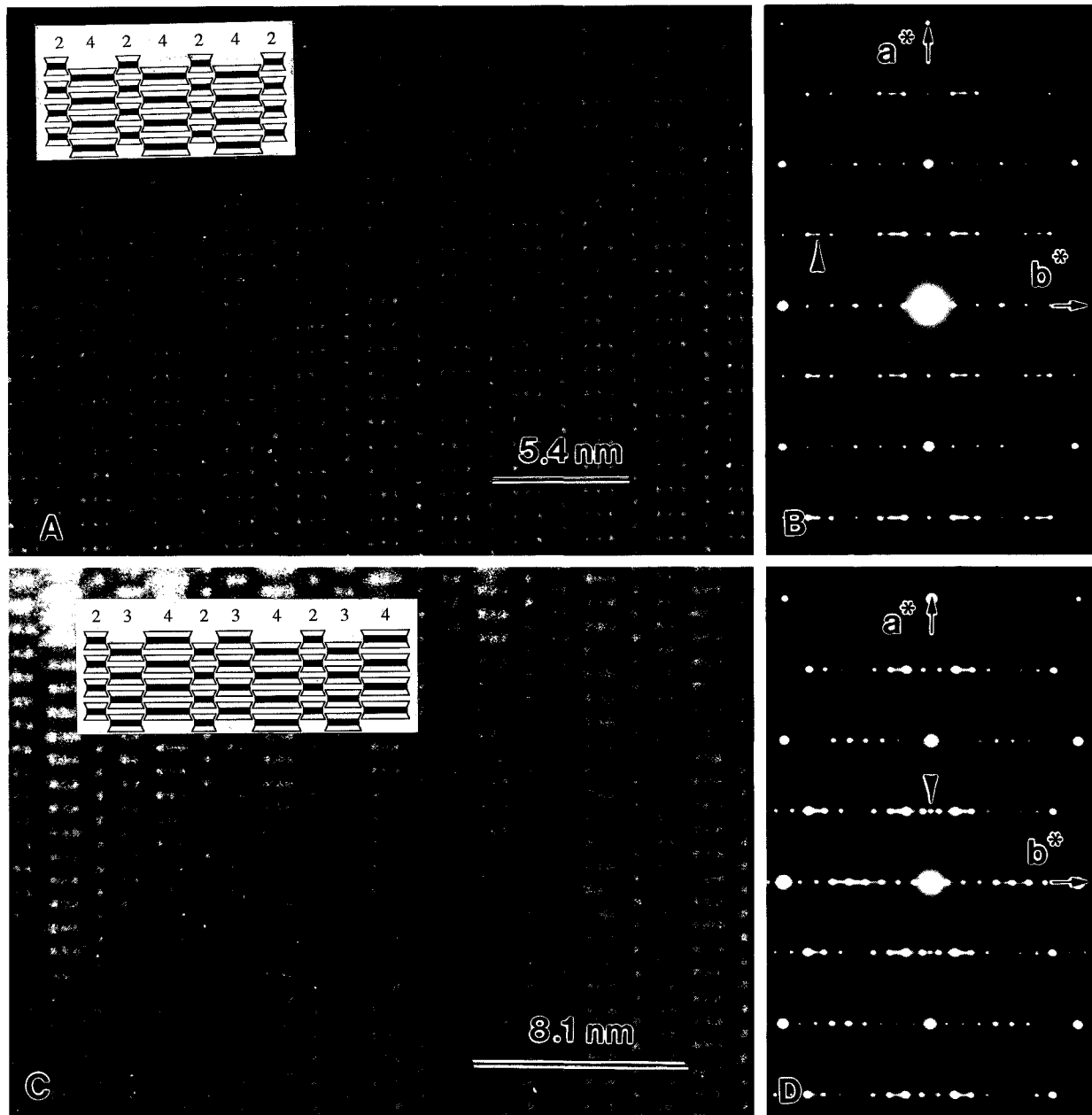
FIGURE 2. HRTEM images and SAED patterns of the [001] zone of the polysome (42) (A and B) and the polysome (234) (C and D). The insets in the images are I-beam representations of the polysomes with the numbers of subchains in each Si tetrahedral chain indicated on top. The arrows in B and D point to diffraction spots belonging to anthophyllite.

(222333) can be represented as $(2^3 3^3)$]. Nonrepetitive sequences are indicated without parentheses (e.g., . . . 23 . . .). The composition of a sequence is given by its modular stoichiometry, e.g., the composition of (423232) is given as $M_{10}P_6 = M_5P_3$.

NEW SHORT-RANGE POLYSOMES BETWEEN AMPHIBOLE AND TALC

The new polysomes found in the samples Mg29a and BL8 can be divided into five groups: polymorphs of ches-

terite, polymorphs of jimthompsonite, polysomes containing pyroxene chains, polysomes with the module stoichiometry M_5P_3, and "giant" polysomes (Table 1).

Chesterite polymorphs

Two polymorphs of chesterite were found in the sample from Alpe Bena. One sequence, (2233), was already observed at Chester, Vermont (Veblen and Buseck 1979). The second chesterite polymorph consists of seven repetitions of the sequence $(2^6 3^6)$ (Fig. 1). The chain sequenc-
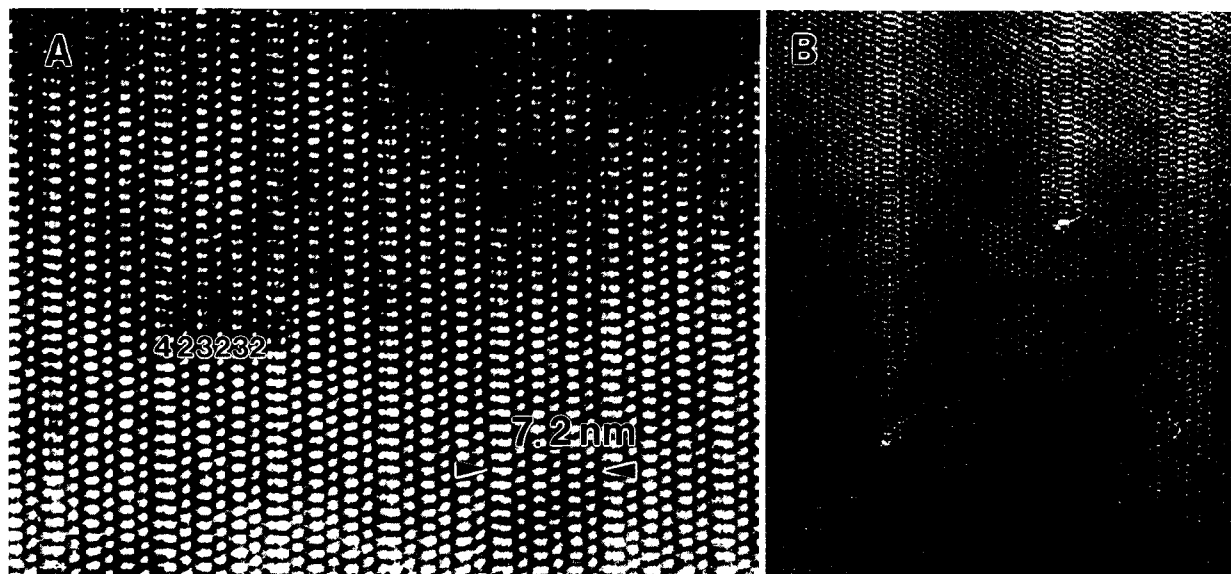
Figure 3. (A) The (423232) polysome. (B) Two zipper terminations in an amphibole slab next to the (423232) polysome. The (324232) zippers are separated by 16 double chains, equal to two repetition lengths of the (423232) polysome. The zipper on the right side has the sequence 323332 and was probably formed from a 324232 sequence.

es following the ordered polysome are similar, but they have isolated chain-width errors. Remarkably, all these errors are compensated. As an example, the isolated triple-chain occurring in one of the sixfold double-chain slabs is compensated by a neighboring triple-chain slab that has only five triple-chains. Such chain-width error compensations are common in chesterite (Veblen and Buseck 1979).

Jimthompsonite polymorphs

Three new jimthompsonite polymorphs, (42), (432), and (4323), were found in the sample from Val Cramosina (Fig. 2). The sequence (42) is the first observed short-range polysome between anthophyllite and talc that contains no triple-chains. An intriguing feature of the (432) polysome is its pronounced asymmetry. A forward (432432) and backward running version (234234) can be distinguished. Faults that change the direction of the sequence, e.g., ... 432432 | 234234 ... , are rare and occur pairwise, and so the original directionality is immediately restored.

(M_5P_3) polysomes

Several tens of unfaulted repetitions of the polysome (423232) with (M_5P_3) stoichiometry are present in the sample Mg29a (Fig. 3A). Terminations show that this polysome is formed directly from anthophyllite without intermediate steps (Fig. 3B). The polysome (332), already found in the Chester rocks, occurs together with the (423232) polysome. The module composition of both polysomes corresponds to a one-to-one mixture of jimthompsonite and chesterite.

"Giant" polysomes

Two giant polysomes were found in the Alpe Bena sample. Both polysomes follow each other along [010] with no interruption by disordered material (Figs. 4A and 4B). Both have the same module stoichiometry ($M_{41}P_{32}$) and the same repetition length (32.85 nm). The structures of the repetition units of both polysomes are similar (Fig. 4C). They contain two faulted sequences with double, triple, and quadruple chains, and two unfaulted sequences of double chains; the second unfaulted double-chain sequence starts at the same position in both polysomes.

POLYSOMES BETWEEN ENSTATITE AND ANTHOPHYLLITE

All ordered biopyriboles found thus far in nature, with the exception of pyroxenes, have compositions along the amphibole-mica join. Thompson (1981) pointed out that there might also exist ordered polysomes between pyroxene and amphibole, especially the polysome (21), a structure consisting of alternating pyroxene and amphibole chains stacked along b. Avgustinik and Vigdergauz (1948) and Sueno et al. (1980), on the basis of X-ray investigations, proposed this structure for an intermediate phase found in the synthetic dehydration products of talc. Konishi and Akai (1991), however, using HRTEM, found a maximum of 10 unfaulted repeats of this (21) sequence, which they considered to result from a random process. Natural hydration of pyroxenes leads mainly to double (1111 → 22) and triple (111 → 3) chains (Yamaguchi et al. 1978; Veblen and Buseck 1981; Nakajima and Ribbe 1980, 1981), but no ordered sequences containing single chains have been observed yet.
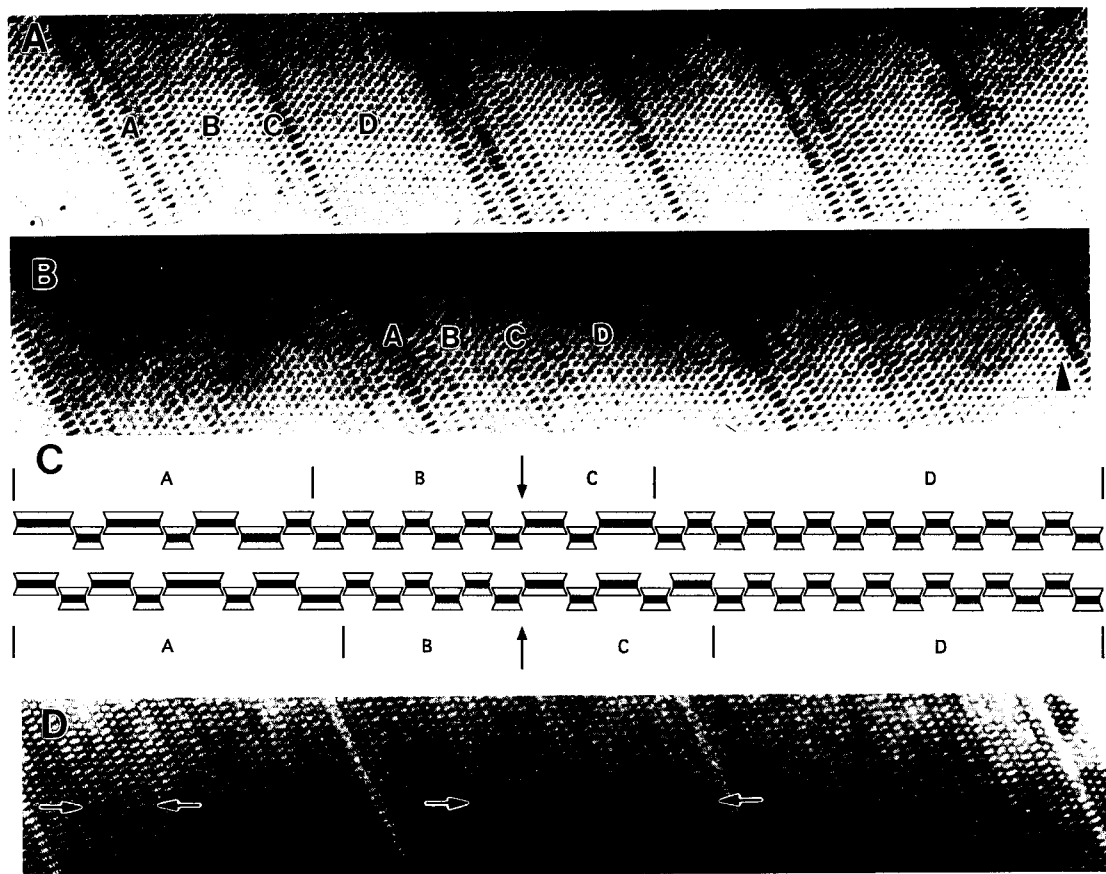
Figure 4. Triple repetition of two giant polysomes: (A) $424233(2)^8324(2)^{15}$ and (B) $32324233(2)^6(32)^3(2)^{12}$. The images are printed as negatives to enhance the contrast. The last faulted sequence in **B** (arrow) is the same as the first faulted sequence in **A**. (C) I-beam representation of both giant polysomes. **A** and **C** indicate the faulted sectors, whereas **B** and **D** are the unfaulted double-chain sequences. The arrows point to the start of the second faulted sequence, which is at the same structural position in both polysomes. (D) Quadruple chains separated by 36 nm or multiples thereof. Ordered (332) polysomes between the quadruple chains are indicated by arrows.

Although optically not visible, inclusions of enstatite several hundreds of nanometers wide occur in antho-phyllite crystals of sample Mg29a. The enstatite grains contain double chains and some rare triple chains. The double-chain slabs are only one I beam wide and 10–20 I beams high along a (Fig. 5A). The terminations are, therefore, all incoherent. A Burgers circuit around a dou-
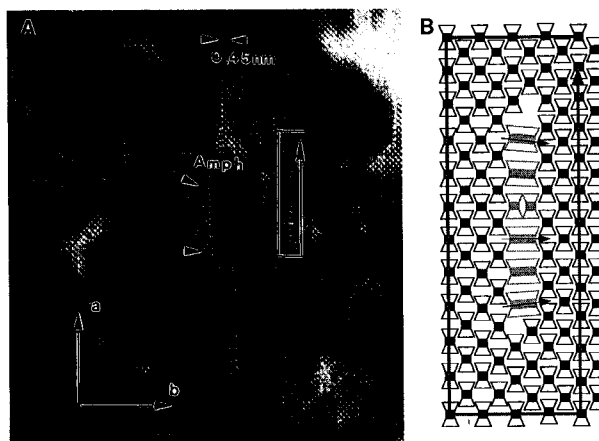
$\longrightarrow$

Figure 5. (A) HRTEM image of an enstatite grain with a high concentration of isolated amphibole zippers. The different contrast on opposite sides of the zippers is due to different strain. Dark areas are under compression, whereas light areas are dilated. The Burgers circuit (arrowed line) around an amphibole zipper indicates that an extra (010) layer of pyroxene I beams (0.91 nm) is introduced on the left side of the zipper. (B) I-beam model of an incoherent, short amphibole zipper in enstatite. The Burgers circuit is shown as a stippled line.
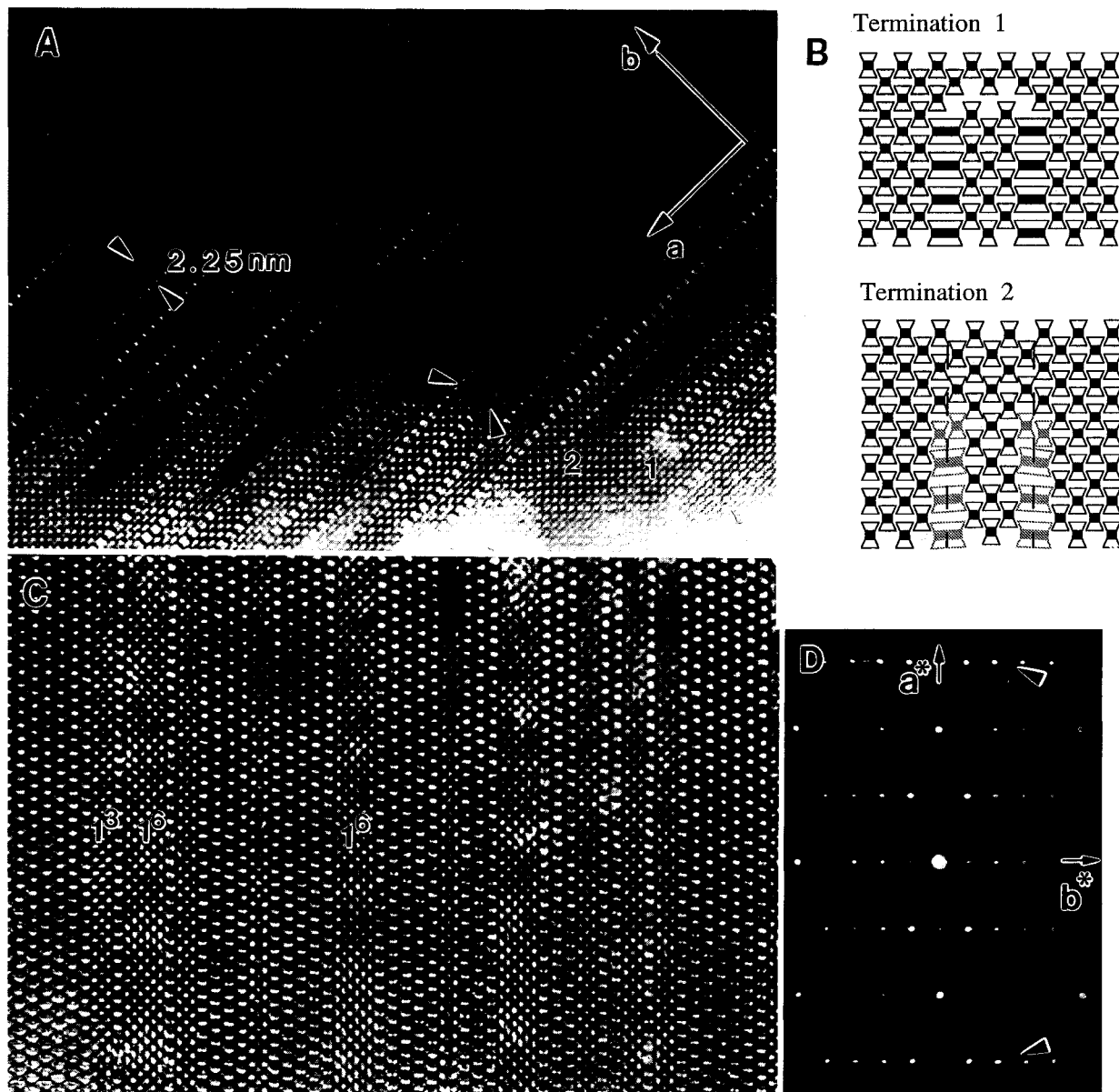
FIGURE 6. (A) HRTEM image of the polysome (2111). Between the arrows the amphibole chains are rotated and the sense of rotation changes from one zipper to the other. The numbers indicate zipper terminations schematically shown in **B**. (B) I-beam models of the terminations: 1 = termination created by a cooperative zipper transformation mechanism; 2 = termination created by the simultaneous propagation of two partial dislocations. (C) Amphibole-pyroxene intergrowth. The pyroxene chains are concentrated in lamellae containing three zippers or multiples of three zippers. (D) The [001] SAED pattern of the (2111) polysome. The arrows point to diffuse reflections doubling the periodicity along [010]. They are strong for rows with $h = 3$ but barely visible for the others. These reflections are probably due to the alternating rotation of the amphibole I beams seen in **A** (see text).

ble-chain fault (Figs. 5A and 5B) shows that the faults connect partial dislocations. Each partial dislocation has a $\frac{1}{4}[100] \pm \frac{1}{3}[001]$ Burgers vector, but only the $\frac{1}{4}[100]$ component is visible in (001) HRTEM images. The $\frac{1}{2}[100]$ offset along the stacking fault juxtaposes two pyroxene I beams, a structural configuration similar to an amphibole I beam. The full offset of $\frac{1}{2}[100]$ along the fault is reached only gradually but the contrast at the ends of the zippers cannot be interpreted unambiguously. It may be due to slightly rotated amphibole I beams or to pairs of pyroxene I beams that are offset by less than $\frac{1}{4}[100]$. The matrix on one side of the zipper is under compression,

whereas the other side is dilated. This stress difference results in strain contrast, which is manifested in the patchy appearance of the image. The same amphibole formation mechanism was proposed for augite of the Balmuccia area, Ivrea zone, northern Italy (Skrotzki et al. 1991). The presence of the relict enstatite and the formation of double chains therein show clearly that the anthophyllite occurring in the bulk rocks of the ultramafic bodies of the Lepontine was formed from enstatite and not vice versa. The high density of dislocations indicates that it was probably formed during a deformation event, most likely during the uplift of the central Lepontine.

In regions with high stacking fault concentrations, ordered sequences appear. The suggested (21) polysome (Thompson 1981) is rare and was not observed to occur with more than five repetitions. Instead, hundreds of (2111) sequences with up to 40 unfaulted repetitions were found in two different enstatite grains (Fig. 6A). This structure represents the first ordered, naturally occurring short-range polysome between amphibole and pyroxene. Chain-width errors in (2111) consist of larger, unfaulted sequences of pyroxene chains, which are not compensated. On the basis of zipper terminations found in (2111), two mechanisms were responsible for the formation of the polysome: the coherent transformations of pyroxene chains (Fig. 6B, termination 1) and the pairwise propagation of partial dislocations (termination 2). The displacements along the two stacking faults have opposite signs and the rotation sense of amphibole I beams alternates from one stacking fault to the next. This alternating rotation of amphibole I beams, which doubles the size of the unit cell along b, could be responsible for the diffuse spots in the (001) diffraction pattern (Fig. 6D) appearing halfway between spots with 2.25 nm periodicity. The diffuse spots were observed in several diffraction patterns that were taken with the aperture exclusively centered above (2111) sequences. In regions where the progress of the transformation of the pyroxene to amphibole is more advanced, the remaining pyroxene chains are arranged in multiples of three. This suggests that the precursor was also a (2111) polysome (Fig. 6C).

The octahedral layers in biopyribole I beams can have two different orientations, designated by + or −. The stacking sequence in orthobiopyriboles such as enstatite is (+ + − −) (Fig. 7A). The introduction of periodic stacking faults five pyroxene chains apart, independent of their shear senses, destroys the initial orthobiopyribole stacking. Displacements of ¼[100] along (010) planes of orthopyroxenes are not equivalent to displacements of −¼[100] (Figs. 7B and 7C). From the two possible sets of alternating shear senses, only one puts two pyroxene chains together with the same orientation of their octahedral sheets (Fig. 7C), which results in the stacking sequence (+ + + − − + − −). To obtain the orthobiopyribole stacking sequence, the orientations of the octahedral layers of two pyroxene chains between stacking faults must be changed. The other set of alternating shear senses juxtaposes pyroxene I beams with different octahedral ori-
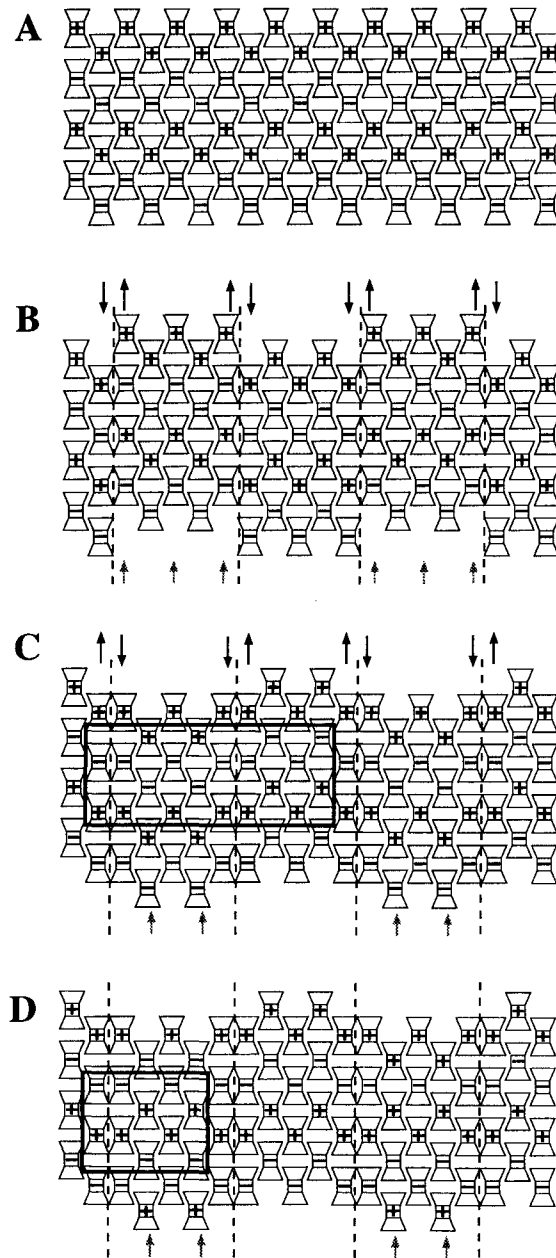

FIGURE 7. (A) Stacking sequence of octahedral sheets in orthopyroxene. (B and C) Stacking sequence after the introduction of periodic stacking faults. The sense of shear changes from one fault plane to the other. Two final configurations are possible. To obtain the orthobiopyribole stacking from these configurations, the orientation of the octahedral layers of all the I beams in the columns marked with gray arrows must be changed. (D) The (2111) polysome with orthopyribole stacking. The unit cells in C and D are outlined.

entations (Fig. 7B). The space group for a (2111) polysome with the orthobiopyribole stacking (+ + − −) is $A2_1ma$, whereas with (+ + + − − + − −) stacking the space group is Am with a doubling of the b parameter (4.5 nm).

TABLE 2. Selected single EMP and AEM analyses

	EMP					AEM					
	Ath Alpe Bena	Che Alpe Bena	Jt Alpe Bena	2σ error	Detection limit (wt%)	Ath Cramosina	Jt Cramosina	(42) Cramosina	(423232) Cramosina	(2111) Cramosina	2σ error
SiO_2	57.65	58.08	58.93	0.4	0.15	58.1	59.5	60.2	59.5	57.2	2.8
Al_2O_3	0.09	0.12	0.19	5.0	0.1	0.66	0.7	0.8	0.6	0.6	28.0
Cr_2O_3	b.d.l.	b.d.l.	0.15	4.1	0.13	n.d.	n.d.	n.d.	n.d.	n.d.	—
FeO	15.28	12.64	10.62	1.4	0.24	9.9	8.3	7.1	7.9	8.0	4.2
MnO	0.11	0.03	0.01	5.0	0.015	0.4	0.1	0.1	0.1	0.19	30.0
MgO	24.81	25.75	26.8	0.5	0.01	27.5	28.1	28.6	28.7	31.22	3.5
NiO	b.d.l.	0.14	0.12	8.5	0.12	n.d.	n.d.	n.d.	n.d.	n.d.	—
CaO	0.28	0.22	0.22	4.2	0.08	0.25	0.3	0.1	0.25	0.24	16.0
Na_2O	b.d.l.	0.04	0.09	8.0	0.06	1.02	0.2	0.3	0.4	1.3	20.0
H_2O	2.16	2.62	2.82			2.1	2.8	2.8	2.5	1.25	
Total	100.57	99.70	99.88			100.0	100.0	100.0	100.0	100.0	
Si	7.99	19.96	11.95			7.94	11.91	11.97	31.81	19.8	
Al	0.014	0.04	0.04			0.11	0.16	0.19	0.39	0.25	
Cr	0.0	0.02	0.02			—	—	—	—	—	
Fe^{2+}	1.49	3.63	1.78			1.13	1.4	1.18	3.52	2.31	
Mn	0.005	0.007	0.002			0.05	0.0	0.0	0.0	0.05	
Mg	5.13	13.19	8.1			5.61	8.41	8.48	22.86	16.11	
Ni	0.01	0.03	0.02			—	—	—	—	—	
Ca	0.04	0.08	0.05			0.04	0.07	0.03	0.16	0.1	
Na	0.0	0.02	0.0			0.27	0.07	0.09	0.39	0.87	
OH	2.0	6.0	4.0			2.0	4.0	4.0	10.0	2.0	

Note: All analyses were normalized according to the module stoichiometries of the polysomes as follows: Ath = $M_7T_8O_{22}(OH)_2$, Che = $M_{17}T_{20}O_{54}(OH)_6$, Jt and (42) = $M_{10}T_{12}O_{32}(OH)_4$, (423232) = $M_{27}T_{32}O_{86}(OH)_{10}$, and (2111) = $M_{19}T_{20}O_{58}(OH)_2$, where M = octahedral sites and T = tetrahedral sites; b.d.l. = below detection level; n.d. = not determined.

This doubling of the b parameter is not observed in SAED patterns, suggesting that the octahedral layers are reoriented during the transformation.

CHEMISTRY OF THE LEPONTINE BIOPYRIBOLES

Only the Alpe Bena samples have homogeneous regions of jimthompsonite and chesterite large enough to allow microprobe analysis. The chemical compositions of the short-range polysomes (42) and (423232) were obtained by AEM. The AEM analyses should be interpreted with care, considering the accuracy of such measurements ($\pm5\%$, Livi and Veblen 1987, Appendix 2 for discussion). The major-element compositions of the Lepontine biopyriboles are similar to those of orthobiopyriboles from the other occurrences (Table 2). Besides the typically reported elements Si, Al, Mg, Ca, Fe, Mn, and Na, some areas contain measurable amounts of Cr and Ni (maximum 0.25 wt%). To facilitate comparison between single measurements, all analyses were normalized to 23 O atoms. The Alpe Bena biopyriboles have Mg contents that are between the values for Chester and Orijärvi biopyriboles, whereas jimthompsonite and chesterite from Val Cramosina have the highest Mg content found thus far (Fig. 8A). AEM analyses of the polysome (42) show Mg contents that overlap with the highest values found in jimthompsomte (Fig. 8B). The composition of the (2111) polysome, determined by AEM, is almost colinear with those of anthophyllite and enstatite from the same sample. Although pyroxenes have nearly twice the fraction of distorted M sites as amphiboles, Fe in coexisting orthoamphibole-orthopyroxene pairs usually prefers the amphibole structure (Trommsdorff and Evans 1972;

Robinson et al. 1982, p. 111). The (2111) polysome follows the same trend: Its X_{Mg} is equal to the value of an equivalent mixture of anthophyllite and enstatite.

FORMATION MECHANISMS OF SHORT-RANGE POLYSOMES

The ordered and disordered wide-chain pyriboles are considered to be intermediate products in the hydration of amphiboles and pyroxenes (Veblen and Buseck 1980). Wide chains are the result of the net displacement of I beams, or parts of them, by $\frac{1}{4}[100] \pm \frac{1}{3}[001]$, accompanied by the addition of water and the removal of octahedral cations (Fig. 9). The detailed mechanism of these displacements, however, is not known. The terminations of wide-chain slabs within anthophyllite are interpreted as frozen in reaction fronts. The terminations are usually coherent and follow the rules given by Veblen and Buseck (1980): (1) The chain sequences on both sides of the termination must have either an even or an odd number of chains. (2) The number of subchains must be equal on both sides of the zipper termination. A change in the number of chains across a termination propagating along a must be accompanied by the transformation of pyroxene modules into mica modules, or vice versa, through the reaction: $nP + 2nH^+ \rightleftharpoons nM + n\,C_o^{2+}$. C_o^{2+} is an octahedral cation and the stoichiometric coefficient n is given by the difference in the number of chains on both sides of the termination (e.g., 222 → 6, n = 2.). Reactions that do not change the number of chains, (e.g., . . . 53 . . . → . . . 44 . . .) are isochemical, but the order of the M and P modules is altered (e.g., . . . MMMMPMMP . . . → . . . MMMPMMMP . . .). The first transformations in antho-
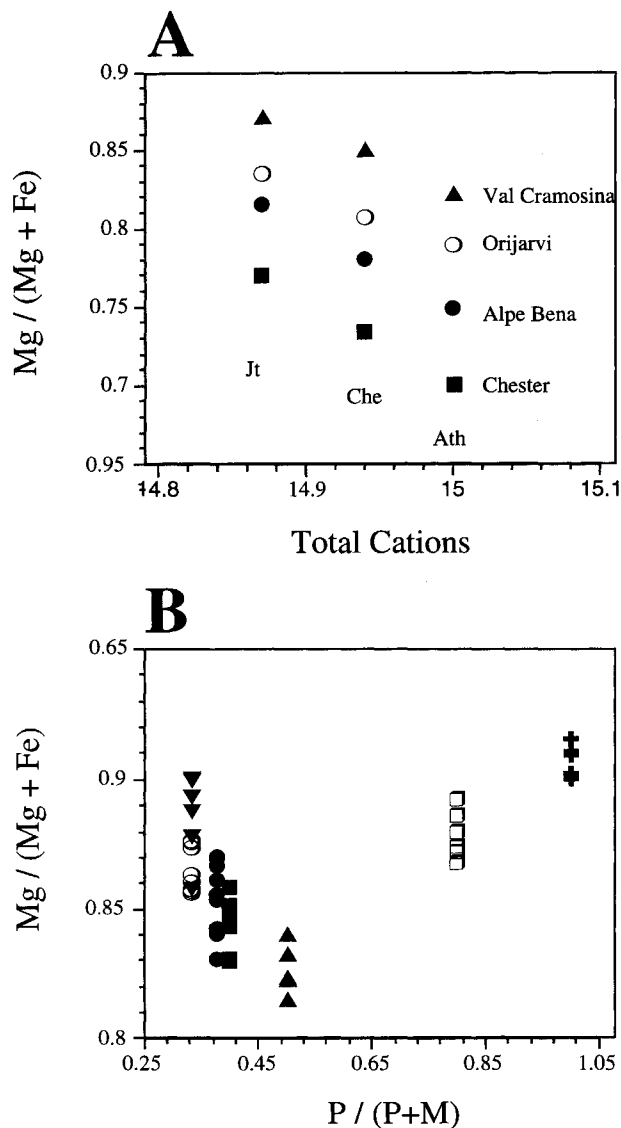
FIGURE 8. (A) Mg/(Mg + Fe) vs. total cations on the M sites of the ordered biopyriboles from Chester (Veblen and Burnham 1978a), Orijärvi (Schumacher and Czank 1987), Alpe Bena and Val Cramosina. (B) Mg/(Mg + Fe) vs. module composition of some short-range polysomes from Alpe Bena and Val Cramosina: triangles = anthophyllite, open circles = jimthompsonite, solid squares = chesterite, inverted triangles = (42), solid circles = (423232), open squares = enstatite, and plus signs = (2111).

FIGURE 9. Schematic representation of the transformation of double chains into triple chains and ordered (42) sequences: (A) ... 222 ... → ... 6 ...; (B) ... 62 ... → ... 44 ...; (C) ... 2442 ... → ... 2424 ...; (D) ... 2442 ... → ... 3333 ... The arrows show the net displacement of I beams or part of them. Reaction A requires the removal of octahedral cations and the addition of H^+ whereas all other reaction steps are isochemical.

phyllite lead to chains wider than triple, such as sextuple and septuple chains (Fig. 9A). The reduction of these wide chains usually results in the formation of (macroscopic) jimthompsonite and chesterite (Figs. 9B and 9C; Grobéty in preparation). The Chester pyriboles, however, give no clue to the formation mechanisms of short-range polysomes or their relationship to the macroscopic pyriboles. No wide-chain terminations related to the formation of short-range polysomes were found. On the basis of the

complex structure of some of the short-range polysomes, Veblen and Buseck (1979) proposed spiral growth about one or several preexisting screw dislocations with a Burgers vector component parallel to [010] as a possible formation mechanism for short-range polysomes. Zippers that progress in the (010) plane would be displaced by the magnitude of the [010] component after each full rotation around the dislocation core. The repetition length of the polysome would be equal to the length of this component. This mechanism is known to operate in the formation of polytypes in layered structures, such as micas (Baronnet 1992) and SiC (Rai et al. 1984). The main problems with this mechanism are the failure to find such screw dislocations in the host amphiboles and the unrealistically large Burgers vectors for some of the dislocations.

Zipper terminations found in or near short range polysomes of the Val Cramosina sample give for the first time direct indications of possible formation mechanisms of short-range polysomes. The (42) polysome, similar to jimthompsonite, is formed through a series of zipper transformations (see Fig. 9). The matrix anthophyllite is first replaced by wide chains, which are reduced to quadruple chains, leading to disordered sequences of quadruple and double chains (Fig. 10A). Instead of reacting to form triple chains, the disordered sequences transform through simultaneous sidestepping of the quadruple and double chains to form the ordered polysome (42) (Fig. 10B). It is not possible to decide whether (42) in this situation is more stable than triple chains or whether the
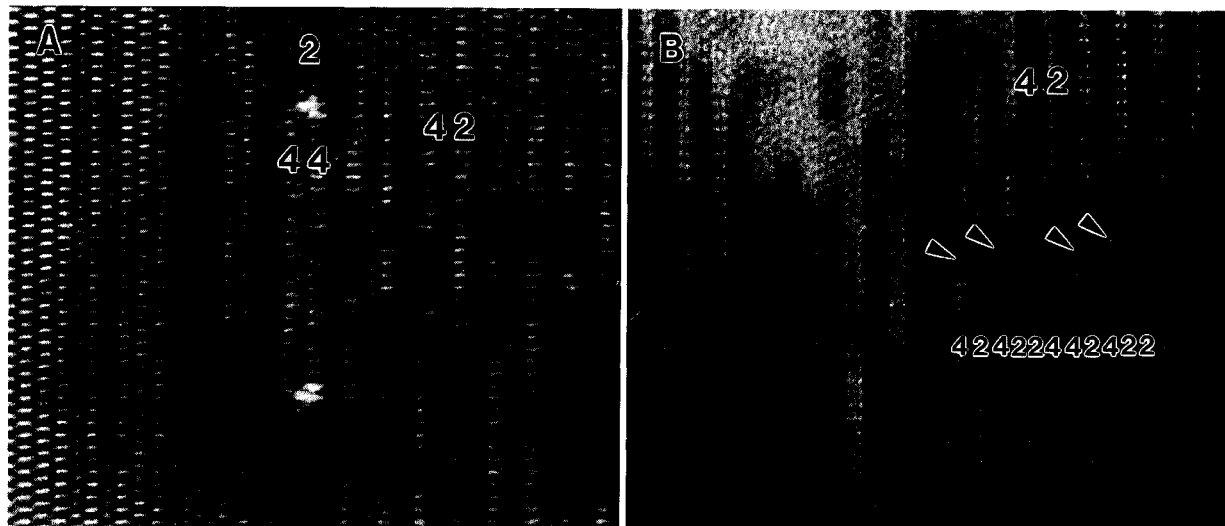
FIGURE 10. (A) A doubly terminated . . . 44 . . . zipper in an anthophyllite lamella near a sequence of the (42) polysome. The widths of the chains at both ends of the zipper cannot be determined with certainty (quintuple or sextuple?). The blurred appearance of the image is due to mechanical drift of the sample during the exposure. (B) Simultaneous sidestepping of double- and quadruple-chain slabs (arrows) transform a disordered sequence of quadruple and double chains into an ordered (42) sequence. The poor contrast at the top of the image is due to the rapid beam damage of the (42) polysome.

appearance of (42) is due only to a lower activation energy for the ordering reaction.

The reaction steps leading to the formation of the other two jimthompsonite polysomes could not be observed directly. The sequence (432) probably has precursor sequences containing quintuple or pyroxene chains, or both. Four equally spaced quintuple chains were found within an otherwise well ordered region of this polysome. The numbers and widths of the chains between the quintuple chains are all the same though their sequences differ (Fig. 11A). The module ratio of this disordered sequence is equal to the module ratio of the polysome (432). A coherent and isochemical transformation of the type . . . 52 → . . . 43 . . . and a subsequent ordering step would lead to the (432) sequence. The same (432) sequence contains several zippers with the sequence (24322122), which has exactly three times the repetition length of (432) (Fig. 11B). The coherent transformation . . . 2122 . . . → . . . 43 . . . converts this sequence into the (432) polysome.

The subsequent zipper transformations . . . 2222 . . . (stoichiometry: M_4P_4) ⇌ . . . 53 . . . (M_6P_2) ⇌ . . . 3212 . . . (M_4P_4) found in an anthophyllite slab next to a region of the (432) polysome (Fig. 11C) might be the link between the presence of quintuple and isolated pyroxene chains within the (432) polysome. This series of terminations within the same zipper differs fundamentally from all other series of zipper terminations observed thus far. Usually, the hydration state within a zipper steadily increases or decreases in one direction. In the above example, however, the hydration state increases with the first termination but decreases back to the hydration state of an amphibole with the second termination. The py-

roxene chain could represent a relict of a previous enstatite grain replaced by anthophyllite. In this case only the quintuple chains would be related to the hydration of the anthophyllite.

Isolated pyroxene chains are also found in the fivefold repetition of the sequence (321222) (Fig. 11D). This polysome may represent a precursor sequence of the jimthompsonite polysome (4323), which has the same repetition length.

The presence of periodically arranged nucleation sites is a possible explanation for the formation of short-range polysomes with large repetition length. Missing amphibole chains, separated by four double chains along a (210) plane, could represent potential nucleation sites for the (423232) polysome (Fig. 12). The repeat periodicity of these defects is exactly half that of the (423232) polysome. These defects could facilitate the displacement of an adjacent double-chain I beam to form a wider I beam. The reason for the periodic repetition of these defects is unclear.

The transformation of ordered sequences may also lead to intermediate polysomes with very large repetition lengths. In the samples studied, only semirandom sequences produced by such a process were observed. They occur as a result of the transformation of the (423232) polysome into the (332) polysome and are characterized by isolated quadruple chains that are separated by 36 nm or some multiple thereof (see Fig. 4D). The sequences between the quadruple chains are nearly perfect (332). The distance that separates the quadruple chains in the semirandom ordered sequence (36 nm) is five times the repetition length of the polysome (423232). The number
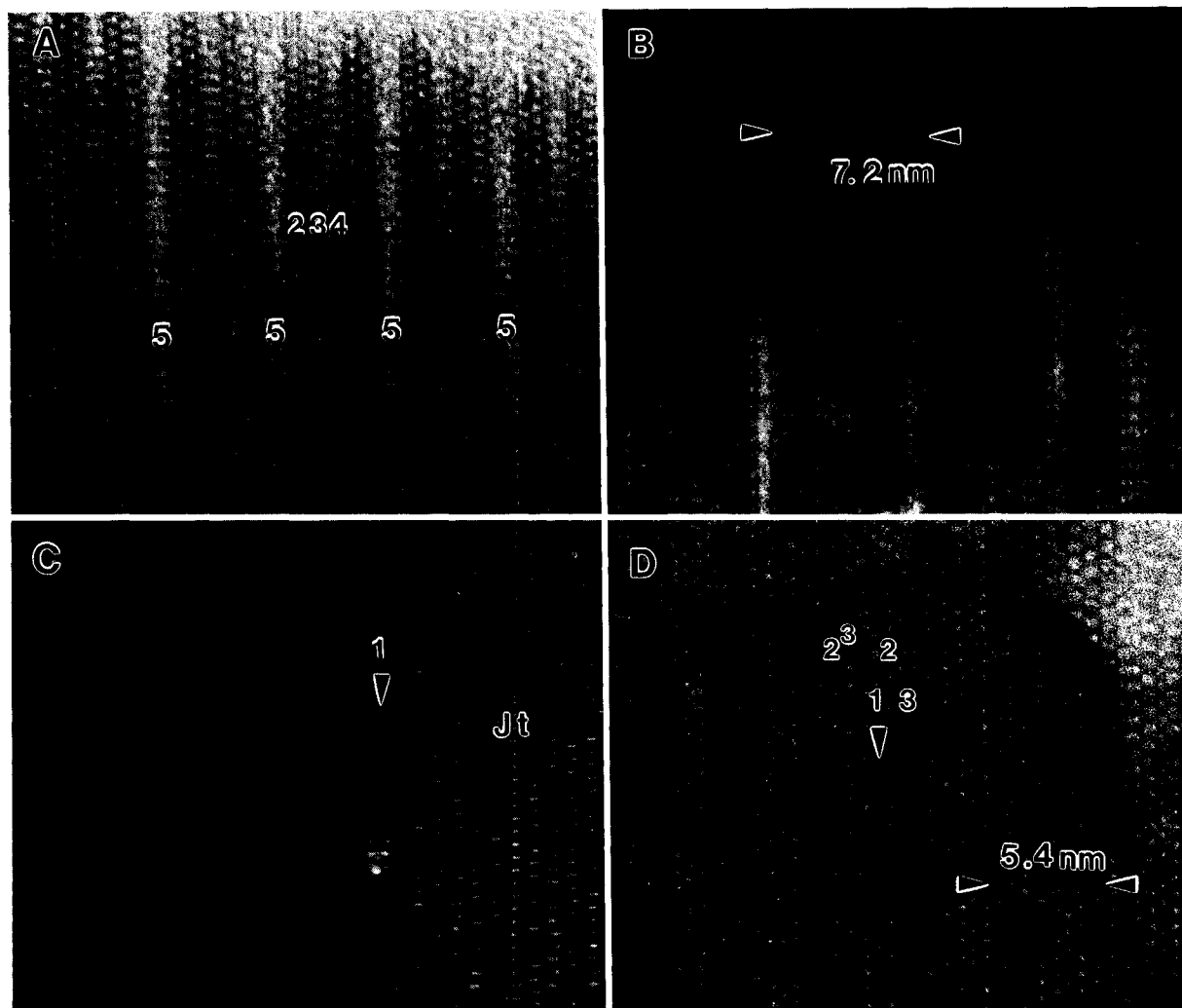
FIGURE 11. (A) Disordered sequence with four equally spaced quintuple chains within the (234) polysome. The slabs between the quintuple chains are disordered sequences composed of one triple, one quadruple, and three double chains. The distance (5.4 nm) between the centers of adjacent quintuple chains is twice the repetition length of the (234) polysome (2.7 nm). (B) Triple repetition of the sequence (22122342). (C) Zipper terminations: . . . 2222 . . . ⇌ . . . 53 . . . ⇌ . . . 2123 . . . There is one quintuple chain at the start of the zipper, which is immediately transformed to . . . 212 . . . . The arrow points along the pyroxene slab in one of the sequences. (D) Quintuple repetition of the polysome (222123).

of modules and the number of chains in polysomes formed by such a process are multiples of the original polysome. The modular stoichiometry $(M_{41}P_{32})$ and the overall number of modules of both giant polyysomes described above contain prime numbers, excluding smaller short-range polysomes as precursors.

The compensated chain-width errors found in the $(2^6 3^6)$ polysome could be an indication that the polysome formed through a chain separation mechanism, by which the double and triple chains of a preexisting chesterite sequence are separated into double- and triple-chain blocks. Zipper transformations that do not change the widths of the individual chains but only their positions within the sequence (sidestepping, Veblen and Buseck 1980; Whittaker et al. 1981, 1982) represent a mechanism for such a chain separation. The sequences containing the errors could represent a stage of reaction in which the separation of double and triple chains is not yet finished. Such a separation mechanism is compatible with the results of lattice-energy calculations (Abbott and Burnham 1991), which suggest that a mixture of jimthompsonite and anthophyllite is more stable than chesterite.

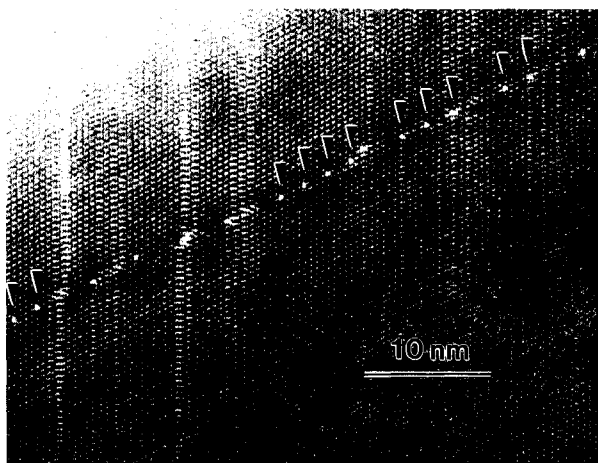Veblen and Buseck (1979) suggested on the basis of phase rule considerations that the occurrence of short-

FIGURE 12. Stacking fault parallel to (210) in a disordered part of the Val Cramosina sample. The displacement has a projected component of $\frac{1}{2}[010]_{Ath}$. All wide-chain zippers are displaced along the fault. They are, therefore, older than the fault. The fault is marked by missing I beams (arrows), which are generally 3.6 nm apart.

range polysome is the result of special growth or reaction mechanisms, but they excluded differences in free energies between polysomes as the driving force for their formation. That is certainly true for complex short-range polysomes, such as the giant polysomes found at Alpe Bena and the polysome (423232). The multiple-step formation of the (42) polysome and the transformation of the (423232) polysome into the (332) polysome, however, suggest that energy minimization may play an important role in the formation of some of the short-range polysomes, even if the resulting phases are not stable relative to the macroscopic biopyriboles.

ACKNOWLEDGMENTS

REFERENCES CITED

Abbott, R.N., Jr., and Burnham, C.W. (1991) Energy calculations bearing on biopyriboles. American Mineralogist, 76, 728–732.

Ahn, J.H., and Buseck, P.R. (1991) Microstructures and fiber-formation mechanisms of crocidolite asbestos. American Mineralogist, 76, 1467–1478.

Ahn, J.H., Cho, M., Jenkins, D.M., and Buseck, P.R. (1991) Structural defects in synthetic tremolitic amphiboles. American Mineralogist, 76, 1811–1823.

Akai, J. (1980) Polymerization process of biopyribole in metasomatism at the Akatani Ore deposit, Japan. Contributions to Mineralogy and Petrology, 80, 117–131.

Avgustinik, A.I., and Vigdergauz, V.S. (1948) Properties of talc during heating. Ogneupory, 13, 218–227.

Baronnet, A. (1992) Polytypism and stacking disorder. In Mineralogical Society of America Reviews in Mineralogy, 27, 231–288.

Berman, R.G., Engi, M., Greenwood, H.J., and Brown, T.H. (1986) Derivation of internally-consistent thermodynamic data by the technique of mathematical programming: A review with application to the system $MgO-SiO_2-H_2O$. Journal of Petrology, 27, 1331–1364.

Buseck, P.R., and Iijima, S. (1974) High resolution electron microscopy of silicates. American Mineralogist, 59, 1–21.

Chisholm, J.E. (1973) Planar defects in fibrous amphiboles. Journal of Materials Science, 8, 475–483.

Cressey, B.A., Whittaker, E.J.W., and Hutchison, J.L. (1982) Morphology and alteration of asbestiform grunerite and anthophyllite. Mineralogical Magazine, 46, 77–87.

Dorling, M., and Zussman, J. (1987) Characteristics of asbestiform and non-asbestiform calcic amphiboles. Lithos, 20, 469–489.

Drits, V.A., Goncharov, Y.I., Aleksandrova, V.A., Khadzi, V.E., and Dimitrik, A.L. (1974) New type of strip silicate. Kristallografiya, 19, 1186–1193 (translated from Soviet Physics—Crystallography, 19, 737–741).

Droop, G.T.R. (1994) Triple-chain pyriboles in Lewisian ultramafic rocks. Mineralogical Magazine, 58, 1–20.

Eggleton, R.A., and Boland, J.N. (1982) Weathering of enstatite to talc through a sequence of transitional phases. Clays and Clay Minerals, 30, 11–20.

Evans, B.W., and Trommsdorff, V. (1974) Stability of enstatite + talc, and CO_{2-} metasomatism of metaperidotites, Val d'Efra, Lepontine Alps. American Journal of Science, 274, 274–296.

Frey, M. (1974) Alpine metamorphism of pelitic and marly rocks of the Central Alps. Schweizerische Mineralogische und Petrographische Mitteilungen, 54, 489–506.

Frey, M., Bucher, K., Frank, E., and Mullis, J. (1980) Alpine metamorphism along the Geotraverse Basel—Chiasso: A review. Eclogae Geologicae Helvetiae, 73, 527–546.

Hutchison, J.L., Irusteta, M.C., and Whittaker, E.J.W. (1975) High-resolution electron microscopy and diffraction studies of fibrous amphiboles. Acta Crystallographica, A31, 794–801.

Johannsen, A. (1911) Petrographic terms for field use. Journal of Geology, 19, 317–322.

Klaper, E.M. (1982) Deformation und Metamorphose in der nördlichen Maggia Zone. Schweizerische Mineralogische und Petrographische Mitteilungen, 62, 47–76.

Konishi, H., and Akai, J. (1991) Depolymerized pyribole structures derived from talc by heating. Physics and Chemistry of Minerals, 17, 569–582.

Köppel, V., Günthert, A., and Grünenfelder, M. (1980) Patterns of U-Pb zircon and monazite ages in polymetamorphic units of the Swiss Central Alps. Schweizerische Mineralogische und Petrographische Mitteilungen, 61, 97–110.

Livi, K.J.T., and Veblen, D.R. (1987) "Eastonite" from Easton, Pennsylvania: A mixture of phlogopite and a new form of serpentine. American Mineralogist, 72, 113–125.

Maresch, W.V., and Czank, M. (1988) Crystal chemistry, growth kinetics and phase relationships of structurally disordered (Mn^{2+}, Mg)-amphiboles. Fortschritte der Mineralogie, 66, 69–121.

Nakajima, Y., and Ribbe, P.H. (1980) Alteration of pyroxene from Hokkaido, Japan to amphibole, clays and other biopyriboles. Neues Jahrbuch für Mineralogie Monatshefte, 6, 258–268.

——— (1981) Texture and structural interpretation of the alteration of pyroxene to other biopyriboles. Contributions to Mineralogy and Petrology, 78, 230–239.

Nissen, H.-U., Wessicken, R., Woensdregt, C.F., and Pfeifer, H.R. (1980) Disordered intermediates between jimthompsonite and anthophyllite from the Swiss Alps. Institute of Physics, Conference Series, 52, 99–100.

Pfeifer, H.-R. (1978) Hydrothermal Alpine metamorphism in metaperidotite rocks of the Cima di Gagnone zone, Valle Verzasca, Switzerland.

Schweizerische Mineralogische und Petrographische Mitteilungen, 58, 400–405.

Pouchon, J.L., and Pichoir, F. (1984) Un nouveau modèle de calcul pour la microanalyse quantitative par spectrométrie de rayon-X: Partie I. Application à l'analyse d'échantillons homogènes. La Recherche Aérospatiale, 3, 167–192.

Price, G. D., and Yeomans, J. (1986) A model for polysomatism. Mineralogical Magazine, 50, 149–156.

Rai, R.S., Korgul, P., and Singh, G. (1984) High resolution electron microscopic studies on a new polytype of SiC and its intergrowth structures. Acta Crystallographica, B40, 132–138.

Robinson, P., Spear, F.S., and Schuhmacher, J.C. (1982) Phase relations of metamorphic amphiboles: Natural occurrence and theory. In Mineralogical Society of America Reviews in Mineralogy, 9B, 1–277.

Schumacher, J.C., and Czank, M. (1987) Mineralogy of triple- and double-chain pyriboles from Orijärvi, southwest Finland. American Mineralogist, 72, 345–352.

Skrotzki, W., Müller, W.F., and Weber, K. (1991) Exsolution phenomena in pyroxenes from the Balmuccia Massif, NW-Italy. European Journal of Mineralogy, 3, 39–61.

Sueno, S., Prewitt, C.T., and Ohmasa, M. (1980) Topotactic decomposition of some silicates. Journal of the Mineralogical Society of Japan, Special Issue 2, 339–363. (Japanese with English abstract)

Stoll, T. (1990) Petrographie und Strukturgeologie um Fusio, Teil 2: Alpe di Röd. Diploma thesis, Eidgenössiche Technische Hochschule, Zurich, Switzerland.

Thompson, J.B., Jr. (1978) Biopyriboles and polysomatic series. American Mineralogist, 63, 239–249.

——— (1981) An introduction to the mineralogy and petrology of the biopyriboles. In Mineralogical Society of America Reviews in Mineralogy, 9A, 141–188.

Trommsdorff, V. (1983) Metamorphose magnesiumreicher Gesteine: Kritischer Vergleich von Natur, Experiment und thermodynamischer Datenbasis. Fortschritte der Mineralogie, 61, 283–308.

Trommsdorff, V., and Evans, B. (1972) Alpine metamorphism of peri-

dotitic rocks. Schweizerische Mineralogische und Petrographische Mitteilungen, 54, 333–354.

Veblen, D.R. (1980) Anthophyllite asbestos: Microstructures, intergrown sheet silicates, and mechanisms of fiber formation. American Mineralogist, 65, 1075–1086.

——— (1991) Polysomatism and polysomatic series: A review and applications. American Mineralogist, 76, 801–826.

Veblen, D.R., and Burnham, C.W. (1978a) New biopyriboles from Chester, Vermont: I. Descriptive mineralogy. American Mineralogist, 63, 1000–1009.

——— (1978b) New biopyriboles from Chester, Vermont: II. The crystal chemistry of jimthompsonite, clinojimthompsonite, and chesterite, and the amphibole-mica reaction. American Mineralogist, 63, 1053–1073.

Veblen, D.R., and Buseck, P.R. (1979) Chain-width order and disorder in biopyriboles. American Mineralogist, 64, 687–700.

——— (1980) Microstructures and reaction mechanisms in biopyriboles. American Mineralogist, 65, 599–623.

——— (1981) Hydrous pyriboles and sheet silicates in pyroxenes and uralites: Intergrowth microstructures and reaction mechanisms. American Mineralogist, 66, 1107–1134.

Whittaker, E.J.W., Cressey, B.A., and Hutchison, J.L. (1981) Edge dislocation in fibrous grunerite. Mineralogical Magazine, 44, 287–291.

——— (1982) Sidestepping of multiple-chain lamellae in grunerite asbestos. Mineralogical Magazine, 46, 273–274.

Yamaguchi, Y., Akai, J., and Tomita, K. (1978) Clinoamphibole lamellae in diopside of garnet lherzolite from Alpe Arami, Bellinzona, Switzerland. Contributions to Mineralogy and Petrology, 66, 263–270.

Yau, Y.-C., Peacor, D.R., and Essene, E.J. (1986) Occurrence of wide-chain Ca-pyriboles as primary crystals in the Salton Sea Geothermal Field, California, USA. Contributions to Mineralogy and Petrology, 94, 127–134.